

# AN OSMOMETER MODEL FOR CHANGES IN THE BUOYANT DENSITY OF CHROMAFFIN GRANULES

S. J. MORRIS AND H. A. SCHULTENS, *Department of Neurochemistry,  
Max-Planck-Institute for Biophysical Chemistry,  
D-3400 Göttingen-Nikolausberg, West Germany, and*

R. SCHÖBER, *Department of Neuropathology,  
Max-Planck-Institute for Brain Research,  
D-6000 Frankfurt-Niederrad, West Germany*

**ABSTRACT** We present a model for the structure of isolated bovine adrenal medulla chromaffin granules derived from the dependence of granule density on the osmotic pressure of the suspension medium at 2°C.

The granule consists of a flexible, inelastic membrane bounding an osmotically active core. The core consists of a solution space and a separate, nonosmotic phase. Since the granule behaves like a "perfect" osmometer over a wide range of osmolalities, we conclude that (a) within these limits, the core consists of a constant amount of condensed material and a constant number of particles in solution, (b) from the constraints of the osmometer model, the osmolality inside the granule must equal the osmolality outside. Therefore the high concentrations of catecholamines (>0.7 M) and ATP (>0.18 M) measured biochemically cannot be dissolved in the core solution as separate molecules, but must be condensed into larger aggregates.

These results are supported by electron micrographic examination of the effect of osmotic pressure changes on granule morphology.

## INTRODUCTION

Chromaffin granules, the subcellular organelles of adrenal medullary cells that store catecholamines, ATP, and protein, can be isolated from medullary tissue and purified by centrifugation methods. (For a critical review see ref. 1). The final step of such a purification usually involves separation by buoyant density either on a sucrose continuous or step gradient or by use of an iso-osmotic gradient (1-3). The latter is preferable since the granules are dehydrated on sucrose gradients, leading to morphological changes and fragility of the purified material.

Iso-osmotic gradient separations of chromaffin granules from their contaminants can be made either by using D<sub>2</sub>O to shift the granule density (2,3) or by using iso-osmotic solutions of varying density of solute. Gradients of the second type can be generated either by varying the concentration of a high molecular weight solute such as glycogen (4) or silica gel (5) in a constant concentration of sucrose, or by making

---

H. A. Schultens' present address is: Department of Physiology, University of Göttingen, D-3400 Göttingen, W. Germany.

gradients of iso-osmotic mixtures of two small molecular weight solutes of differing density (2).

Iso-osmotic density gradients of the first type were first introduced by de Duve and collaborators (6,7) to probe the osmotic properties of mitochondria and lysosomes. They used glycogen to shift the density of the solution without raising the osmotic pressure. Laduron (4) extended the use of this type of gradient to adrenal medullary mitochondria and chromaffin granules and demonstrated that granules increase their density in response to increases in osmolality of the gradient medium. Lagercrantz et al. (5) used colloidal Ludox silica to show the same phenomenon. Neither of these methods were useful for purification since contaminating mitochondria overlapped the granules in the 300–350 mosM range, the range at which the granules exist *in vivo*.

Morris and Schovanka (2) have employed iso-osmotic, 300 mosM gradients of sucrose and metrizamide to separate the granules from contaminating mitochondria and lysosomes. By varying the osmotic pressure of these gradients from 260 to 1,800 mosM, they have confirmed the behavior of granules as osmometers qualitatively and have demonstrated that at physiological osmolalities, granules contain a large water space.

The following report is a rigorous analysis of the osmotic properties of the granules. We develop a three-compartment model for granule structure from the osmometer model originally proposed by de Duve et al. (6) and show that the chromaffin granules behave like good osmometers over the range of osmolalities studied. The question of whether the granules are permeable to sucrose and the implications for the structure of the biological materials stored at high concentrations in the core are discussed.

## METHODS

All methods used in this study have been described in detail elsewhere (2,8). All solutions were buffered with 20 mM Na-HEPES, pH 7.2.

The crude granule fraction used as the starting material for the gradient separation was prepared from bovine adrenal glands placed on ice within 30 min, and processed within 1.5 h of the death of the animals.

Linear iso-osmotic continuous gradients of sucrose and metrizamide were generated in Lusteroid tubes for the Beckman SW 41Ti rotor (Beckman Instruments, Inc., Spinco Div., Palo Alto, Calif.). These were loaded with 1.5 ml of the crude granule material resuspended in 0.300 osM sucrose and centrifuged 1.5 h at 32,500 rpm (129,000 *g*-av), sufficient to establish equilibrium. The gradients were fractionated by piercing the bottom of the tube and collecting ~0.5-ml fractions.

The peak of granule activity was found by assaying fractions for ATP by the firefly luciferin-luciferase assay (9). The refractive indexes of the gradient fractions were read at 580 Å with an Abbé-type refractometer thermostatted at 0–1°C, and the density of the granule peak tube, determined from plots of the density and refractive index of the solutions used to form the gradients, assuming linear mixing. Since the gradients were only analytic, the contaminating mitochondria and lysosomes were no problem even when they overlapped the distribution of the granules.

Densities of the gradient solutions at 0°C were read by micropycnometry. The osmolalities of the solutions were read on a Knauer semimicro freezing point depression osmometer.

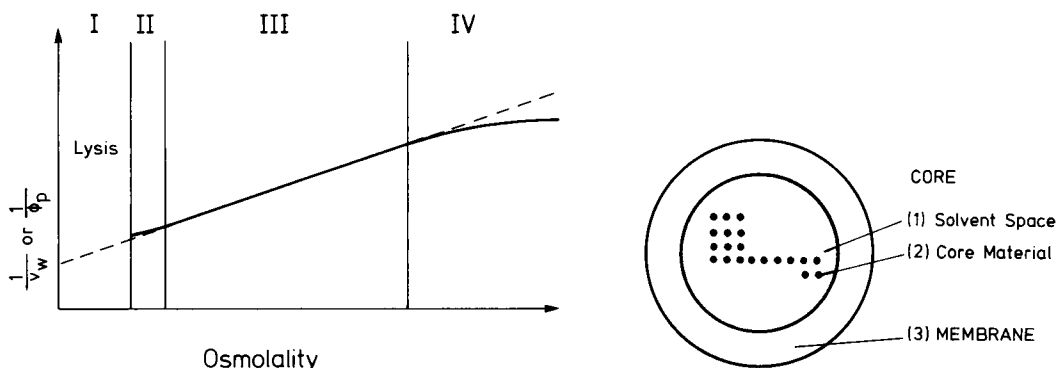


FIGURE 1 Changes in reciprocal total volume ( $\phi_p$ ) and the water space ( $v_w$ ) of a membrane-bound perfect osmometer as a function of the osmolality of the suspension medium. In the region in which the particles behave as perfect osmometers (region III), the reciprocal plots are linear with the extrapolated  $y$ -intercepts of 0 for the reciprocal total volume and 1 for the reciprocal water space. See text for further details.

FIGURE 2 Schematic representation of the three-compartment model used to represent the osmotic properties of the chromaffin granule. The granule is modeled as a semi-permeable membrane bag of volume fraction  $v_s$  enclosing a core space; the latter is subdivided into the solvent space ( $v_w$ ) and the core material space ( $v_c$ ). See text for further details.

All calculations were performed on a PDP 11/40 computer (Digital Equipment Corp., Maynard, Mass.) with a GT/40 graphics display with FORTRAN IV and assembler programs.

## THEORY

### *Chromaffin Granules as Osmometers*

Cells and subcellular particles often behave as osmometers, i.e. their densities depend on the osmotic pressure in the surrounding medium (4,6,7). We may picture the behavior of a biological osmometer (an osmotically active core surrounded by a flexible, inelastic membrane) as noted in Fig. 1, where a function of the reciprocal water space is plotted against osmolality of the suspension medium. The particle has qualitatively different behavior depending upon the osmotic pressure: (a) The osmotic pressure of the suspending medium is too low and the particles rupture. (b) At low osmotic pressure, the membrane is stretched taut and is of limited elasticity, like a well-inflated football, and the osmotic pressure inside the granule is higher than outside. (c) The osmotic pressure inside is the same as outside. The granule acts as a perfect osmometer. (d) Increasing the osmolality does not lead to a corresponding decrease in volume. Either the core structure prevents the particle from collapsing completely or the osmotically active solute in the core becomes too concentrated to act as an ideal solute (ideal gas); the particle approaches its minimum volume.

We will proceed to develop a model to explain the behavior of a particle as a "perfect" osmometer. The theory is modified from de Duve et al. (6), to whom the reader is referred for greater detail.

We imagine the chromaffin granule to consist of three compartments (Fig. 2): the core, subdivided into an osmotically active solvent space, a space for core material, and the membrane.

"Solvent" is defined as a medium that can pass freely through the membrane and does not interact with the solute inside or outside the membrane. The core material includes the osmotically active solute that generates osmotic pressure inside the granule and cannot pass through the membrane, and any solid, nonosmotic material the granule may contain. The core material compartment and the membrane may contain nonosmotically active solvent. Under the conditions we assume, the solutes inside and outside the membrane act as ideal gases. The granule responds to osmotic pressure much like a football or balloon in a pressure chamber.

If we denote  $\phi$  = volume,  $\mu$  = mass, and  $\rho$  = density,

$\mu_s, \phi_s, \rho_s$  = mass, volume, and density of the membrane; all are constant except for possible water of hydration. (Substitution of D<sub>2</sub>O for H<sub>2</sub>O could change the mass and density of the shell and core material).

$\mu_c, \phi_c, \rho_c$  = parameters for the core material depleted of osmotically active solvent.

$\mu_{sol}, \phi_{sol}, \rho_{sol}$  = parameters for the osmotically active portion of the core material (core solute).

$\mu_w, \phi_w, \rho_w$  = parameters for the solvent contained in the core.

$\mu_p, \phi_p, \rho_p$  = parameters for the whole particle.

$m$  = molality (mosmol/g) of the solution outside the granule.

For a perfect osmometer, the osmolality inside the granule is the same as outside. In the following, we assume that this means that the molalities are equal (*vide infra*). If we define  $A$  as the fraction of the core material which is osmotically active

$$A = \mu_{sol}/\mu_c, \quad (1)$$

then the volume of the solvent space

$$\phi_w = A\mu_c/\rho_w m = \phi_c A\rho_c/m\rho_w, \quad (2)$$

and the mass of solvent contained in the solvent space:

$$\mu_w = A\mu_c/m, \quad (3)$$

from which we can calculate the density, since

$$\mu_p = \mu_s + \mu_c + \mu_w = \mu_s + \mu_c(1 + A/m), \quad (4)$$

$$\phi_p = \phi_s + \phi_c + \phi_w = \phi_s + \phi_c(1 + A\rho_c/m\rho_w). \quad (5)$$

Therefore,

$$\begin{aligned} \rho_p &= \frac{\mu_s + \mu_c(1 + A/m)}{\phi_s + \phi_c(1 + A\rho_c/m\rho_w)} = \frac{\rho_s + B\rho_c(1 + A/m)}{1 + B(1 + A\rho_c/m\rho_w)} \\ &= \rho_w \frac{AB\rho_c + (B\rho_c + \rho_s)m}{AB\rho_c + (1 + B)m\rho_w}. \end{aligned} \quad (6)$$

Where we have defined

$$B = \phi_c / \phi_s = \text{constant}, \quad (7)$$

we can rewrite Eq. 6 in the simpler form,

$$\rho_p(m) = \rho_w(1 + p_1 m) / (1 + p_2 m), \quad (8)$$

where we define the parameters  $p_1$  and  $p_2$  as

$$p_1 = (B\rho_c + \rho_s) / AB\rho_c, \quad (9a)$$

$$p_2 = (1 + B)\rho_w / AB\rho_c. \quad (9b)$$

We can now give the volume fractions for the various compartments of the particle. We have

$$v_s + v_c + v_w = 1, \quad (10)$$

$$\rho_s v_s + \rho_c v_c + \rho_w v_w = \rho_p, \quad (11)$$

and from Eq. 5 we obtain

$$v_s + v_c(1 + A\rho_c / m\rho_w) = 1 \quad (12)$$

From Eq. 10 it follows that

$$v_w = AB\rho_c / (AB\rho_c + (1 + B)m\rho_w), \quad (13)$$

which can be rewritten as

$$1/v_w = 1 + p_2 m, \quad (14)$$

from Eq. 9b above.

Eq. 14 shows that plots of  $1/v_w$  vs. molality should give straight lines in the region where the particle acts like a perfect osmometer (Fig. 1). Similarly, one can show that plots of  $1/\phi_p$  vs. molality should also give straight lines in this region, and an extrapolated  $y$ -intercept of 0. Not only does this result allow us to test the fit of the model to the experimental data, but it provides a theoretical basis upon which to judge the results of the osmotic dependence of the water space made directly on the granules by the methods described above and by morphometry.

## RESULTS AND DISCUSSION

### *Osmotic Pressure-Induced Changes in Buoyant Density*

The buoyant density of chromaffin granules at varying osmolalities was assessed on iso-osmotic sucrose-metrazamide density gradients as described above. The results of 54 determinations at osmolalities ranging from 236 to 1,680 mosM are presented in Fig. 3. The solid curve represents the best fit to the data (see below). Although it was possible to determine the density of granules below 300 mosM, the recovery of ATP

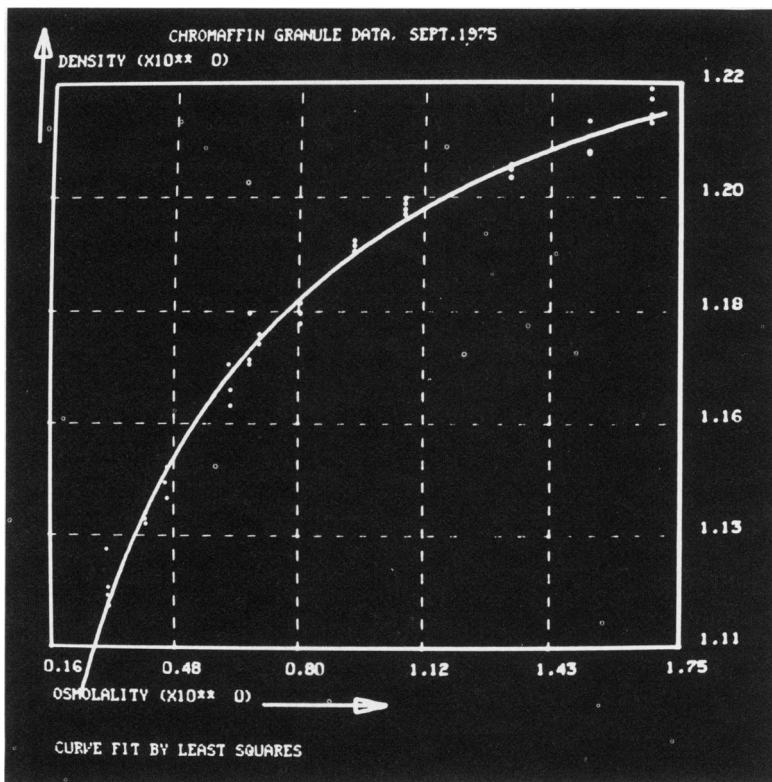


FIGURE 3 Buoyant density of chromaffin granules as a function of the osmotic pressure of the suspension medium. The buoyant density of the granules was measured on iso-osmotic sucrose/metrizamide density gradients as described in the Methods section. The plot was photographed on the GT44 display screen after the least squares best fit of Eq. 8 was obtained.

in the granule peak dropped rapidly as the osmolality was reduced, suggesting that the granules were lysing and the density measured represents a subset of granules able to withstand the hypotonic conditions. Above 300 mosM very little ATP was lost from the granule peak.

#### *Fitting the Theoretical Model to the Data*

To apply the theory developed above to the data, it is necessary to convert osmolality to molality with Eq. 50 below.

**DIRECT FIT TO THE DENSITY-OSMOTIC PRESSURE DATA (METHOD A)** Eq. 6 defines  $\rho_p(m)$  as a function of two independent parameters. Fitting to the data set of Fig. 3 gives the values

$$p_1 = 3.4286 \quad \text{and} \quad p_2 = 2.6979. \quad (15)$$

The fact that Eqs. 1-5 lead to an expression for  $\rho_p(m)$  containing only two independent parameters means that there is a basic mathematical ambiguity in the three-

compartment model of the perfect osmometer as originally formulated (6). We may in principle pick any physically possible values of  $A$ ,  $B$ ,  $\rho_c$ , and  $\rho_s$  which satisfy Eqs. 9a and 9b with the values given by Eq. 15. Values of  $A$  and  $\rho_c$  on the hyperbola

$$A\rho_c = k = \text{constant}, \quad (16)$$

such that the value

$$\rho_s = B(p_1 k - \rho_c) \quad (17)$$

is positive, will leave Eqs. 1 and 8–11 unchanged. This ambiguity means that many specific models satisfy the theory and give the same relationship of density to osmotic pressure. For example, a simple magnification, i.e. multiplying all extensive quantities by the same factor, gives the same  $p_1$  and  $p_2$  because  $A$ ,  $B$ ,  $\rho_c$ , and  $\rho_s$  are not changed. Any particle models that give the same values for  $p_1$  and  $p_2$  will be completely equivalent, i.e., they will give the same curve  $\rho_p(m)$ .

A simple way to explore the various possible models allowed by the theory is to combine the quantities  $A$ ,  $B$ ,  $\rho_c$ , and  $\rho_s$  to suit a particular interpretation.

Consider a particle spherical for at least one value of the osmotic pressure,  $m_0$ , at which the theory is valid. If the particle radius is  $R$ , the volume is

$$\phi_p = (4/3)\pi R^3. \quad (18)$$

If the membrane thickness  $t \ll R$ , then, approximately,

$$\phi_s = 4\pi R^2 t, \quad (19)$$

from which we obtain (for that osmolality)

$$v_s = \phi_s/\phi_p = 3t/R. \quad (20)$$

Since  $v_w$  is known from Eq. 14, we can also specify  $v_c$  as

$$v_c = 1 - v_s - v_w = 1 - 3t/R - 1/(1 + p_2 m_0). \quad (21)$$

This gives  $B$  as

$$B = \phi_c/\phi_s = v_c/v_s. \quad (22)$$

One of the three remaining quantities  $A$ ,  $\rho_c$ , and  $\rho_s$  must be specified. The membrane density is most accessible to measurement; if we take this as given, we can solve Eqs. 9a and 9b for  $A$  and  $\rho_s$ :

$$\rho_c = [\rho_w(1 + B)p_1/p_2 - \rho_s]/B, \quad (23)$$

$$A = (1 + B)\rho_w/B\rho_c p_2. \quad (24)$$

Taking the dimensions for a spherical granule to be  $R = 1,800 \text{ \AA}$  and shell thickness  $65 \text{ \AA}$  at the osmolality  $m_0 = 0.360$ ,<sup>1</sup> we obtain

<sup>1</sup> Morris, S. J., R. Schober and M. Hellweg, unpublished observations.

$$v_s = 0.1083, v_w = 0.5167, v_c = 0.3750, B = 3.462. \quad (25)$$

From experiment,  $\rho_s = 1.162$  g/ml (8). With water as the solvent,  $\rho_w = 1.000$  g/ml. This yields

$$\rho_c = 1.302 \text{ g/ml}, A = 0.3668. \quad (26)$$

If we can assume that the osmotically active core material has the same bulk density as the inert core material, we can use Eq. 1 in the form:

$$A = \mu_{\text{sol}}/\mu_c = \phi_{\text{sol}}/\phi_c = v_{\text{sol}}/v_c, \quad (27)$$

$$v_{\text{sol}} = 0.138. \quad (28)$$

Therefore the osmotically active solution in the core occupies a total volume fraction of

$$v_w + v_{\text{sol}} = 0.6542. \quad (29)$$

This solution space should not be confused with the (smaller) water space  $v_w$  (see below).

Another hypothetical case of interest is a granule with a completely dissolved or colloiddally disperse core ( $A = 1$ ). Solving Eqs. 9a and 9b for  $\rho_c$  with  $\rho_s = 1.162$  and  $\rho_w = 1$  yields

$$\rho_c = 1.645, B = 0.2908. \quad (30)$$

For a spherical particle at 0.360 osM, we can use Eqs. 21 and 22 to calculate

$$v_s = (1 - v_w)/(B + 1) = 0.3269, \quad (31)$$

using  $v_w$  from Eq. 25. Eq. 20 then gives a membrane thickness ( $t$ ) of 196 Å for a radius of 1,800 Å, or for a membrane thickness of 65 Å, a particle radius of 596 Å, showing that the postulate of a completely dispersed core is not consistent with current measurements of granule size or membrane thickness.

Other specific models may be derived from the general theoretical model, but without experimental values for the core density or structure it is difficult to avoid arbitrariness.

**FITTING TO THE RECIPROCAL WATER SPACE (METHOD B)** The statistical analysis of curve fitting is most readily applied to the fitting of a linear regression line (10). A criterion that the particle being investigated is a perfect osmometer is that the reciprocal water space varies linearly with the osmotic pressure (Eq. 14). This can be seen from a simple two-compartment model, the first compartment being the water space of volume  $\phi_w$ , the second being everything else that belongs to the particle (total mass  $\mu_d$ , volume  $\phi_d$ , both independent of the osmotic pressure). The second compartment is then the particle depleted of osmotically active solvent. Let  $\alpha$  be the fraction of  $\mu_d$  that is osmotically active:

$$\alpha = \mu_{\text{sol}}/\mu_d. \quad (32)$$



As above, we obtain

$$\phi_p = \phi_d(1 + \alpha\rho_d/\rho_w m); \quad (33)$$

therefore

$$1 = v_d(1 + \alpha\rho_d/\rho_w m) \quad \text{or} \quad v_d = 1/(1 + \alpha\rho_d/\rho_w m). \quad (34)$$

The water space,

$$v_w = 1 - v_d = \alpha\rho_d/(\rho_w m + \alpha\rho_d), \quad (35)$$

$$1/v_w = 1 + (\rho_w/\alpha\rho_d)m = 1 + bm, \quad (36)$$

where

$$b = \rho_w/\alpha\rho_d = \text{constant}. \quad (37)$$

Using

$$\mu_p = \mu_d + \mu_w = \mu_d + \alpha\mu_d/m = \mu_d(1 + \alpha/m), \quad (38)$$

we obtain

$$\rho_p = \rho_d\rho_w(\alpha + m)/(\alpha\rho_d + m\rho_w). \quad (39)$$

Rearranging, we obtain

$$(\rho_w/\alpha\rho_d)m = (\rho_p - \rho_w)/(\rho_d - \rho_p). \quad (40)$$

Setting Eq. 36 in Eq. 40 yields

$$1/v_w = (\rho_d - \rho_w)/(\rho_d - \rho_p) \quad (41)$$

This is the desired transformation function for the data  $\rho_p(m)$ .

The parameter  $\alpha$  does not appear explicitly in Eq. 41. We therefore used the following method to determine both  $\rho_d$  and  $\alpha$  from a straight line fit to data transformed by Eq. 41: trial values for  $\rho_d$  were inserted into Eq. 41 and the transformed values for the dependent variable were calculated. To these values as a function of osmolality, a straight line of the form

$$y = bx + a \quad (42)$$

was fit by the least squares method. That value of  $\rho_d$  was accepted which gave  $a = 1$  as the  $y$ -intercept, in agreement with Eq. 36. We then obtain

$$\alpha = \rho_w/b\rho_d \quad (43)$$

from Eq. 37.

At the same time, a statistical analysis of variance (10, 11) was carried out on the transformed data (see Fig. 4). Though the data obviously follows a straight line over most of its course, it was found that the noise in the data would not allow us to establish the limits of perfect osmometer behavior (linearity of the transformed data) conclusively. Eliminating points from the left to determine the boundary of region II in

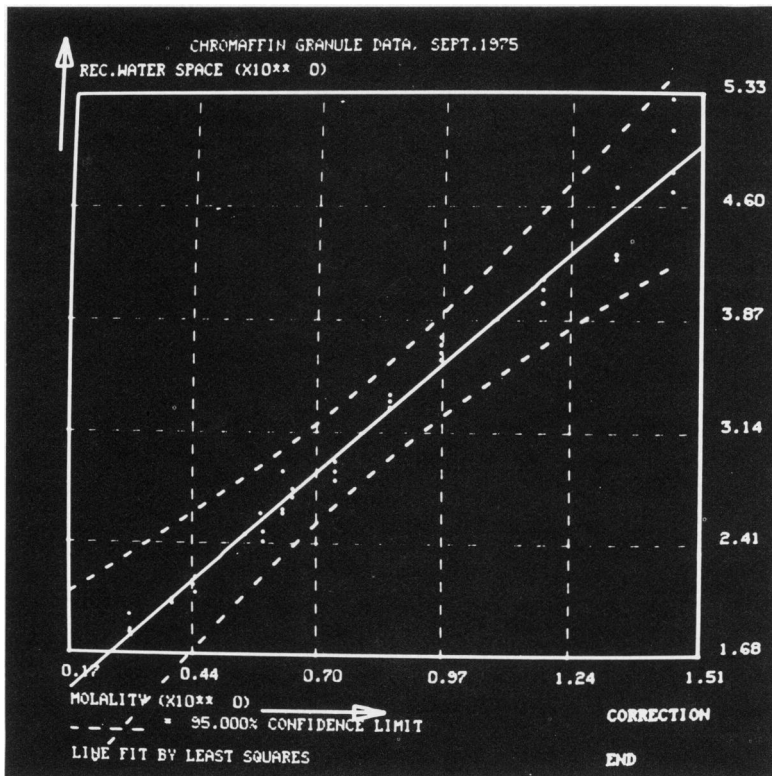


FIGURE 4 Reciprocal water space ( $1/v_w$ ) of chromaffin granules as a function of osmotic pressure. The data of Fig. 3 was transformed according to Eq. 41. The plot was photographed on the GT44 display screen after fitting the least squares straight line. The dashed lines represent the 95% confidence interval. cf. Method B in the Results and Discussion section for more details.

Fig. 1 at first led to a monotonic decrease in Fisher's F-test ratio to below the  $P = 0.05$  level at molality  $m = 0.272$ , but this test for linearity became indeterminate as more points were eliminated. The boundary of region IV in Fig. 1 also could not be determined because of noise in the data.

The best fit through all of the data gave

$$\rho_d = 1.2725, b = 2.65 \pm 0.42, a = 1.0 \pm 0.38, \alpha = 0.297. \quad (44)$$

**COMPARISON OF METHODS A AND B** Since methods A and B are two somewhat different approaches to the data analysis, a translation of the results of B to the form of A gives a comparison of the methods and a test of their reliability.

Comparing Eq. 14 with Eq. 36, we see that the slope of the regression line and the parameter  $p_2$  from the fit to the density data should have the same value. We obtain

$$b = 2.65, p_2 = 2.70. \quad (45)$$

These are in good agreement within the standard deviation given in Eqs. 44. In addi-

tion, one can compare the value for the density of the depleted granule from method B with the asymptotic value from method A:

$$\rho_d = 1.2725, \rho_w p_1 / p_2 = 1.2708. \quad (46)$$

The mass of osmotically active solute in the particle per gram of depleted particle by method B is given in Eq. 44. From method A, this is calculated to be

$$\alpha = A\mu_c / (\mu_c + \mu_s) = AB\rho_c / (B\rho_c + \rho_s) = 1/\rho_1 = 0.292, \quad (47)$$

using Eqs. 7 and 9a. Furthermore, one can reverse the transformation Eq. 41 and transform the regression line to a curve of density vs. osmolality. The values deviated from the fitted curve of method A by at most 0.01%.

**MOLARITY, MOLALITY, AND OSMOLALITY** The molarity (molar concentration)  $c$ , defined as the number of millimoles of a solute in a cubic centimeter of solution, is related to the molality  $m$ , defined as the ratio of the mass of solute to mass of solvent in a given volume, by an equation given by de Duve et al. (6):

$$m = c/\rho_w(1 - Vc), \quad (48)$$

where  $\rho_w$  is the density of the solvent and  $V$  is the partial specific volume of the solute. For aqueous sucrose solutions, de Duve et al. (6) find that a value of  $V = 0.21$  fits the data well. No temperature is explicitly stated for this value, but judging by Table 3 of that paper, 20°C is probably meant. This corresponds well with more recently published data (12).

Osmolality, usually measured by freezing point depression or osmosity, is in general not equal to molality. However, an equation of the form of Eq. 48 is quite useful to convert molarity to osmolality. Eq. 48 can even be used to convert concentration at one temperature to molality or osmolality at another temperature. We have fit Eq. 48 to data from tables for aqueous sucrose solutions (10) to convert molarity at 20°C to osmolality determined by freezing point depression. Using  $\rho_w = 0.99823$  for water at 20°C, we find

$$V = 0.3087, \quad (49)$$

to fit the data given with an error of less than 0.7%. We caution against interpreting  $V$  as a true partial specific volume in this case, however.

To convert osmolality to molality, we fit a function of the form

$$m = \frac{\text{osM} + p_3 \cdot \text{osM}^2}{p_1 + p_2 \cdot \text{osM}}, \quad (50)$$

to tabulated data for sucrose solutions (10). We obtain

$$p_1 = 1.0058, p_2 = 0.0730, p_3 = -0.0164, \quad (51)$$

which reproduce the data with an error of less than 1.2%.

In all cases, Eq. 50 was used to convert osmolality to molality before applying the theory to the data.

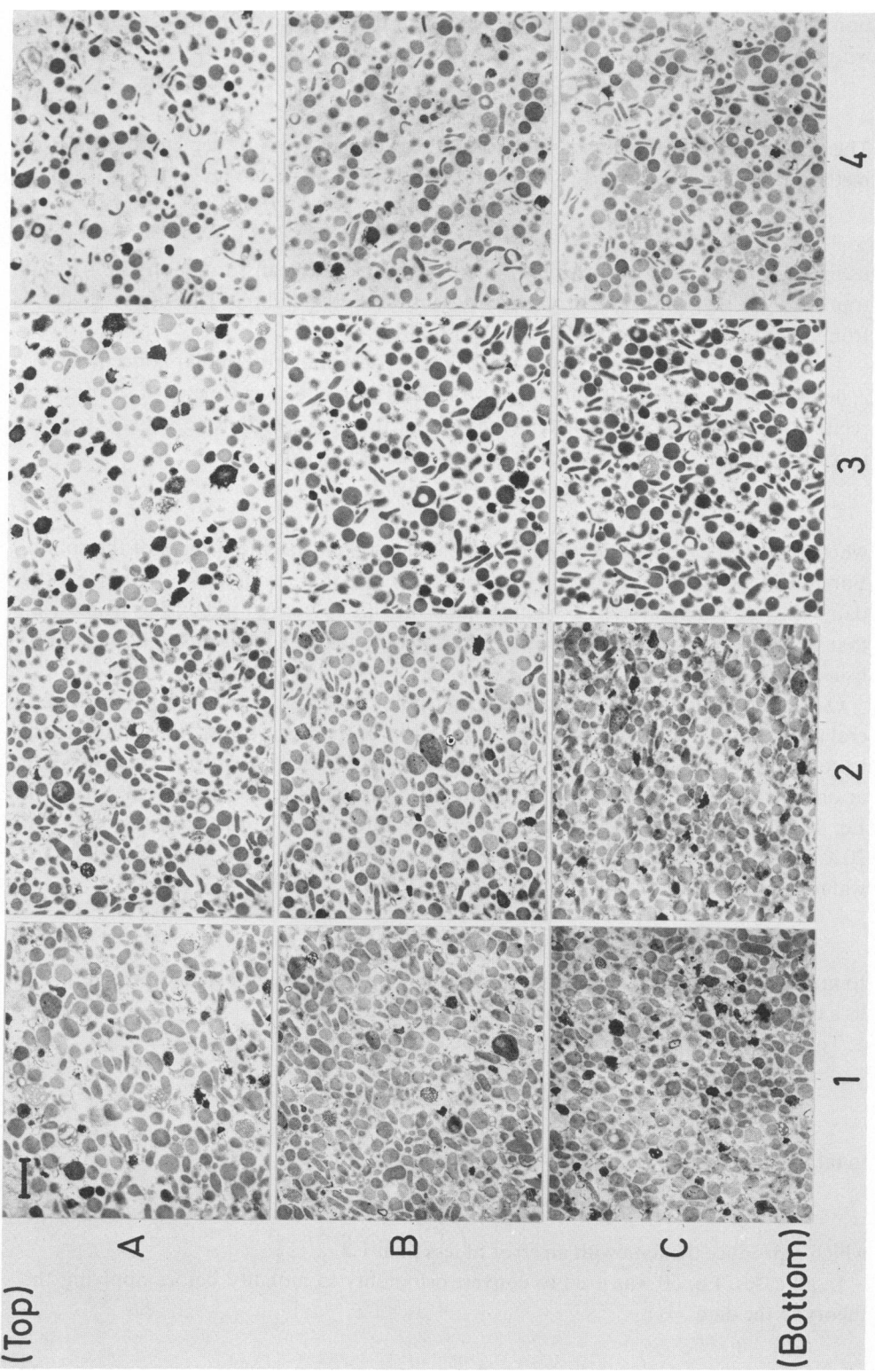


TABLE I  
ESTIMATES OF CHROMAFFIN GRANULE VOLUME FRACTIONS

Reference	Method	Osmolality of suspension medium	Volume fractions*				Bound water	Water space ( $v_w$ ) accessible to sucrose	
			$v_w$	$v_c$	$v_s$	$v_c + v_s$			
						Hydrated			Dehydrated
							% of total	%	
This study	Iso-osmotic density gradient	0.360	0.516	0.375	0.108	0.483		0	
4	"	0.300	0.525†			0.482§	0.329	21.4° <sub>o</sub>	22.8° <sub>o</sub>
2	D <sub>2</sub> O/H <sub>2</sub> O exchange	0.280	0.63				0.37		
13	Exclusion of radio-labeled solutes	0.360						30° <sub>o</sub>	10.8° <sub>o</sub>
14	"	0.300	0.60				0.40		
15	Wet wt/dry wt	0.360	0.685				0.315		

\*Cf. Eq. 10.

†Osmotic space + sucrose space.

§Dehydrated core and membrane volume fraction + bound water volume fraction.

### *Electron Microscopy*

The crude granule fraction was resuspended in ice-cold 360 osmol sucrose at high concentration and equal aliquots were added to 100 vol of 360, 600, 900, and 1,200 mosM sucrose and incubated for 1 h at 0°C. The granules were fixed in 1% glutaraldehyde, centrifuged into pellets, stained with OsO<sub>4</sub> and lead citrate, and prepared for electron microscopic examination as described elsewhere (8). Care was taken to orient the pellets so that sections were cut parallel to the gravitational field, allowing a top-to-bottom examination of the pellet along the centrifugal force gradient. The section was photographed at 15 approximately equidistant intervals from top to bottom. The results are presented in a photomontage, where fields taken at points ranging from the top, middle, and bottom of each pellet are shown (Fig. 5). The 360-mosmol pellet is typical of the crude granule material discussed in detail elsewhere (8). Most of the contaminating mitochondria and lysosomes are confined to the upper strata of the pellet. Chromaffin granules appear as membrane-bound round or ovoid particles 2,000–5,000 Å in diameter, with dense-staining cores. As the osmotic pressure is increased, the granules appear to be smaller on the average and many elongated forms, either disks or cups, are seen. The annular shapes which occur in the higher osmolalities probably result from cups cut perpendicular to their axis of symmetry. This in turn implies that many of the round or oval profiles seen in these pellets result from other

FIGURE 5 Electron micrographs of chromaffin granules subjected to sucrose solutions of various osmolalities for 1 h at 0°C before fixation and preparation for examination in the electron microscope. The results of typical fields taken near the top (A), middle (B), and bottom (C) of the pelleted material from the samples treated with (1) 0.36, (2) 0.60, (3) 0.90, and (4) 1.20 osM sucrose solutions. See Electron Microscopy in Results and Discussion for further details. Black scale bar represents 0.5  $\mu$ m.

planes of section through collapsed granules and therefore that most of the granules have been transformed into flattened structures by the increased osmotic pressure.

#### *The Water Space*

As can be seen in Table I, estimates of the water space are in the range 0.5–0.7. Those methods based upon exchange of deuterated or tritiated water or other labeled compounds (2, 13, 14) or by difference between wet and dry weight (15) are on the order of 20–30% larger than the two measurements made using the various forms of the osmometer model. We attribute these discrepancies to the fact that the tracer experiments measure all water that can be exchanged during the period of the measurement, including some of the “obligate” water of hydration. Phillips et al. (13) reach a similar conclusion from their measurement of granule bulk water space by a tracer method.

#### *The Sucrose Space*

A number of authors have suggested that the chromaffin granule membrane is permeable to various small ions and molecules. Carlsson and Hillarp (16) claim that the membrane is freely permeable to KCl and sucrose; however, several recent communications refute these claims. Salt permeability has been shown to be quite selective (17–20) and as Perlman (21) and Phillips et al. (13) point out, the protracted stability of granules in isotonic (0.3–0.35 osmol) sucrose solutions suggests that this molecule is impermeant. Perlman (21) has shown that the stability of granules decreases as a function of the number of carbons in the sugar residue. Granules are stable in C<sub>6</sub> sugars at 0°C but lyse in C<sub>5</sub> and C<sub>4</sub> sugars.

Laduron (4) has calculated a sucrose-permeable space of 0.12, using the model originally proposed by de Duve et al. (6) for mitochondria. We have analysed our data on the null hypothesis that the granules are impermeable to sucrose, and as noted above get an excellent fit to our model. To ascertain the scope of the validity of this assumption, we propose two alternative cases: (a) A sucrose space exists, permeable to sucrose but not metrizamide. (b) The sucrose space is permeable to both solute molecules. The merits of these cases may be decided in principle by comparing Laduron's results with ours (Table I). Laduron used glycogen gradients containing a constant concentration of sucrose while our sucrose-metrizamide has a continually varying sucrose concentration. If the sucrose space = 0.12, for a granule of  $\rho = 1.122$  at 0.25 M sucrose, the calculated change in density of 0.002 due to the inclusion of only sucrose is not within the accuracy of either Laduron's or our results. At a much higher sucrose concentration of 1.316 M, our calculations predict a particle density of 1.219, indistinguishable from the value given by Laduron (cf. Fig. 18 of ref. 4). A similar set of arguments would apply if metrizamide were also permeable. Therefore we can conclude that, within the precision of the measurements, the sucrose space cannot be larger than 0.12. The data of Phillips et al. (13) give a sucrose-permeable space of 15% of the total water space, as measured by exchange of radiolabeled inulin, sucrose, and HTO. This is somewhat lower than Laduron's data, which would yield

a value of  $\sim 23\%$ . Correcting the 15% figure for inclusion of obligate water (see previous section) reduces it to  $\sim 11\%$ .

### *Granule Structure*

The basic limitation of the three-compartment model is its dependence upon assumptions for the size and shape of the granules and the calculational errors which will result if the values chosen are inaccurate. However, the model does provide a good first approximation of the granule structure as a particle bound by semi-permeable membrane having a highly hydrated and easily deformable core material. The ultramicrographic observations not only provide confirmation of these findings but demonstrate that the particles collapse into disks rather than minimize their surface areas by becoming smaller spheres, therefore confirming the assumption that the membrane is both flexible and inelastic.

The good fit obtained for the data to the perfect osmometer model over a wide range of osmolalities supports the observations of the selective permeability of the membrane to water versus small sugars and alcohols (21) and various cations including protons (17–20).

Chromaffin granules are estimated to contain more than 0.7 M catecholamine, 0.18 M ATP, 0.25 M  $\text{Ca}^{2+}$  and  $\text{Mg}^{2+}$ , and 3 mM protein of 80,000 mol wt (1,13). Since a perfect osmometer at equilibrium has the same concentration of particles inside as outside, for the particles to exist at physiological osmolalities, the stores of catecholamine and ATP must be condensed or aggregated to reduce the internal osmotic pressure far below the estimated 0.7–1.0 osM. Pletscher and collaborators have presented evidence that catecholamine ATP and calcium can condense into aggregates of 2,000–10,000 mol wt (22). Our results suggest that only about 35% of the core solute exists as a low molecular weight colloid, the remainder being condensed into an osmotically inert form.

The core density of 1.30 is consistent with a high protein concentration; however, the simplifying assumption that the osmotically active and inactive core fractions have the same bulk density (Eq. 27) precludes any rigorous analysis of this result. Thus the underlying molecular structure of the granule core storage complex remains to be elucidated.

We wish to thank Mr. I. Schovanka for his excellent technical assistance.

*Received for publication 30 March 1977.*

### REFERENCES

1. WINKLER, H., and A. D. SMITH. 1975. The chromaffin granule and the storage of catecholamines. *Handb. Physiol.: Endocrinol.* **6**:321.
2. MORRIS, S. J., and I. SCHOVANKA. 1977. Some physical properties of adrenal medulla chromaffin granules isolated by a new iso-osmotic density gradient procedure. *Biochim. Biophys. Acta.* **464**:53.
3. TRIFARÓ, J. M., and J. DWORKIND. 1970. A new and simple method for isolation of adrenal chromaffin granules by means of an isotonic density gradient. *Anal. Biochem.* **34**:403.

4. LADURON, P. 1969. Biosynthèse, Localisation Intracellulaire et Transport des Catecholamines, Ph.D. thesis Catholic University, Louvain, France.
5. LAGERCRANTZ, H., H. PERTOFT, and L. STJÄRNE. 1970. Facts and artifacts in gradient centrifugation analysis of catecholamine granules. *Acta Physiol. Scand.* **78**:561.
6. DE DUVE, C., J. BERTHET, and H. BEAUFAY. 1959. Gradient centrifugation of cell particles; theory and application. *Prog. Biophys. Chem.* **9**:325.
7. BEAUFAY, H., and J. BERTHET. 1963. Medium, composition and equilibrium density of subcellular particles from rat liver. *Biochem. Soc. Symp.* **23**:66.
8. MORRIS, S. J., R. SCHÖBER, and H. A. SCHULTENS. 1977. Correlation of physical and morphological parameters with release of catecholamines, ATP and protein from adrenal medulla chromaffin granules. *Biochim. Biophys. Acta.* **464**:65.
9. DOWDALL, M. J., A. F. BOYNE, and V. P. WHITTAKER. 1973. Adenosine triphosphate: a constituent of cholinergic synaptic vesicles. *Biochem. J.* **140**:1.
10. COLQUHOUN, D. 1971. Lectures on Biostatistics. Clarendon Press, Oxford, U.K.
11. DIEM, K., editor. 1962. Documenta Geigy Scientific Tables. 6th edition. Geigy, Ardsley, N.Y. 146-196.
12. WEAST, R. W., editor. 1972. Handbook of Chemistry and Physics. 54th edition. CRC Press, Cleveland, Ohio. D-229.
13. PHILLIPS, J. H., Y. P. ALLISON, and S. J. MORRIS. 1977. The distribution of calcium, magnesium, copper and iron in the bovine adrenal medulla. *Neuroscience.* **2**:147.
14. KIRSHNER, N., C. HOLLOWAY, and D. L. KAMIN. 1966. Permeability of catecholamine granules. *Biochim. Biophys. Acta.* **112**:532.
15. HILLARP, N-Å. 1959. Further observations on the state of the catecholamines stored in the adrenal medullary granules. *Acta Physiol. Scand.* **47**:271.
16. CARLSSON, A., and N-Å HILLARP. 1958. On the state of the catecholamines of the adrenal medullary granules. *Acta Physiol. Scand.* **44**:163.
17. JOHNSON, R. G., and A. SCARPA. 1976. Internal pH of isolated chromaffin vesicles. *J. Biol. Chem.* **251**: 2189.
18. DOLAIS-KITABGI, J., and R. L. PERLMAN. 1975. The stimulation of catecholamine release from chromaffin granules by valinomycin. *Mol. Pharmacol.* **11**:745.
19. CASEY, R. P., D. NJUS, G. K. RADDA, and P. A. SEHR. 1976. ATP-evoked catecholamine release in chromaffin granules: osmotic lysis as a consequence of proton translocation. *Biochem. J.* In press.
20. PAPADOPOULOU-DIAFOTIS, Z., S. J. MORRIS, and R. SCHÖBER. 1977. Differential lysis of adrenaline and noradrenaline chromaffin granules promoted by the ionophore BrX537A. *Neuroscience.* **2**:609.
21. PERLMAN, R. L. 1976. The permeability of chromaffin granules to non-electrolytes. *Biochem. Pharmacol.* **25**:1035.
22. PLETSCHER, A., M. DA PRADA, K. H. BERNEIS, H. STEFFEN, B. LÜTOLD, and H. G. WEDER. 1974. Molecular organization of amine storage organelles of blood platelets and adrenal medulla. *Adv. Cytopharmacol.* **2**:257-264.